

Impact of Active vs. Passive Robot Behavior on Task Efficiency in Collaborative Physical HRI

Original

Impact of Active vs. Passive Robot Behavior on Task Efficiency in Collaborative Physical HRI / Tiozzo, A., Azzarà, G.S., Rizzo, A., Sciutti, A., Rea, F.. - In: IEEE ROBOTICS AND AUTOMATION LETTERS. - ISSN 2377-3766. - 10:11(2025), pp. 11291-11298. [10.1109/lra.2025.3609942]

Availability:

This version is available at: 11583/3003892 since: 2025-10-13T09:43:02Z

Publisher:

IEEE

Published

DOI:10.1109/lra.2025.3609942

Terms of use:

This article is made available under terms and conditions as specified in the corresponding bibliographic description in the repository






Publisher copyright

IEEE postprint/Author's Accepted Manuscript

©2025 IEEE. Personal use of this material is permitted. Permission from IEEE must be obtained for all other uses, in any current or future media, including reprinting/republishing this material for advertising or promotional purposes, creating new collecting works, for resale or lists, or reuse of any copyrighted component of this work in other works.

(Article begins on next page)

Impact of Active vs. Passive Robot Behavior on Task Efficiency in Collaborative Physical HRI

Alessandro Tiozzo , Giulia Scorza Azzarà , *Member, IEEE*, Alessandro Rizzo , *Senior Member, IEEE*, Alessandra Sciutti , *Member, IEEE*, and Francesco Rea , *Member, IEEE*

Abstract—Advancements in physical Human-Robot Interaction (pHRI) aim to achieve natural and efficient collaboration between humans and robots, especially in dynamic environments where task performance is essential. This study focuses on co-manipulative human-robot joint activities, exploring key components of performance and synchronization. The primary objective was to design an active control technique for the iCub robot’s arms that enhances task efficiency with a distinct approach than traditional force feedback controls. Comparing an iCub’s passive behavior with the designed active one has registered an increase in its contribution, given through adaptive velocity and mimicry, and showcasing its ability to respond dynamically to changes in human actions. Furthermore, a measurement of the exertion applied by the counterparts revealed that the active behavior required greater energy consumption to reach those levels of synchronization and performance. These results highlight the implications of balancing active behavior with effort intensity to achieve task efficiency in pHRIs.

Index Terms—Human-robot collaboration, humanoid robot systems, cooperating robots.

I. INTRODUCTION

PROGRESS in physical Human-Robot Interaction (pHRI) technology has focused on creating and deploying robots

Received 8 June 2025; accepted 9 August 2025. Date of publication 15 September 2025; date of current version 22 September 2025. This article was recommended for publication by Associate Editor Federica Ferraguti and Editor Angelika Peer upon evaluation of the reviewers’ comments. This work was supported in part by the Brain and Machines Flagship of the Italian Institute of Technology, in part by a Starting through from the European Research Council (ERC) through the European Union’s H2020 Research and Innovation Programme, under Grant 804388, wHiSPER, and in part by the Project Future Artificial Intelligence Research (FAIR), code PE000013 funded by the European Union - NextGenerationEUPNRR MUR - M4C2 - Investimento 1.3 - Avviso. Creazione di “Partenariati estesi alle università, ai centri di ricerca, alle aziende per il finanziamento di progetti di ricerca di base”. (*Corresponding author: Alessandro Tiozzo.*)

This work involved human subjects or animals in its research. Approval of all ethical and experimental procedures and protocols was granted by the Regional Ethics Committee (Protocol: IIT_INT_HRI).

Alessandro Tiozzo is with the Department of Control and Computer Engineering (DAUIN), Polytechnic of Turin, 10129 Turin, Italy, and also with CONTACT Unit, Italian Institute of Technology (IIT), 16163 Genoa, Italy (e-mail: alessandro.tiozzo@iit.it).

Giulia Scorza Azzarà is with the Department of Robotics (DIBRIS), University of Genoa, 16145 Genoa, Italy, and also with the RBCS Unit, Italian Institute of Technology (IIT), 16163 Genoa, Italy (e-mail: giulia.scorza@iit.it).

Alessandro Rizzo is with the Department of Electronics and Telecommunications (DET), Polytechnic of Turin, 10129 Turin, Italy (e-mail: alessandro.rizzo@polito.it).

Alessandra Sciutti and Francesco Rea are with the CONTACT Unit, Italian Institute of Technology (IIT), 16163 Genoa, Italy (e-mail: alessandra.sciutti@iit.it; francesco.rea@iit.it).

that can engage in efficient and natural collaboration with humans [1]. A crucial aspect of these interactions is to achieve a state of togetherness and coordination, similar to the synchronization observed between human peers in collaborative tasks [2]. Such synchronization is enhanced through mimicry, which smooths interactions and fosters mutual liking between human partners [3] and between human-robot couples [4]. Another parameter to be considered is the performance of the task, an essential indicator of the effectiveness of joint actions. Task performance is influenced by factors such as coupling stiffness and the skills of human and robotic partners [5]. The stiffness of the coupling, in particular, plays a key role in the quality of haptic feedback, affecting overall task performance. In fact, high coupling stiffness can improve precision and stability [6], while robot adaptability to human partner skills can lead to more intuitive and flawless collaboration [7]. The stiffness in a robotic agent’s joint is managed by compliance, which enables the end-effector position to be perturbed at each point of its trajectory. Different compliance levels can classify different roles of the robot in the interaction, and prior investigation shows how role exchanging enhances perturbation robustness during interactions [8] and improves the performance [9]. Moreover, socially aware movements by the robotic agent can significantly improve the quality of the interaction [10]; thus, active behavior can lead to greater participation of the human partner [11].

In previous research, a joint sawing action performed through a non-rigid interface (e.g., a flexible wire) has been proposed to study collaborative interactions with the iCub robot. In particular, how engaging in joint actions might affect human visuospatial attention by redirecting it toward the robot’s hand [12]. During that coordinative activity, the robot’s passive behavior adopted the joint position’s control with fixed stiffness and damping coefficients in the impedance controller, experimentally determined to ensure safety and slight adaptation during collaboration. However, users quickly adapted to the task during an experiment in which such a demeanor was exerted. The participants also tried to increase their movement speed, which the iCub robot could not match, disrupting coordination smoothness. In fact, non-adaptive behavior has been studied to lead to a significant reduction in the rhythm of the performed activity [13]. This highlights the need for a controller design that facilitates the adaptivity of the iCub to the pace of the participants, as discussed in [14].

In-depth analysis [15] has identified specific kinematic elements that are crucial to facilitating the creation of a cyclical

exchange of forces that highlights the collaboration between the human and the robot, reminiscent of cooperative tasks typically performed among human dyads [16]. Those elements include expanding the range of motion size, enhancing mutual cooperation among peers, and extending the robot hand trajectory into the human peripersonal space, the immediate area surrounding the body where objects can be reached and interacted with. This space is crucial for predicting human movements and ensuring safe, natural collaboration. This approach is intended to improve task efficiency by enabling smoother, more synchronized interactions [17].

Furthermore, it has been shown how robot adaptability, especially in collaborative physical tasks, significantly impacts how the robotic agent is perceived and relied on [18], [19]. Some studies have already involved variability of motor stiffness in cooperation with unpredictable human responses. Still, they were more focused on manipulations concerning physics contacts with the robotic limb or end-effector [20], while the case study involved in our research implies a non-rigid tool (e.g., a flexible wire) to interface the partners. In pHRI, force feedback is typically required for this process. However, humanoid robots like the iCub, which use motorized cables to actuate their joints, are challenging to control using force feedback due to the compliance and non-linearities introduced by the cable-driven actuation system [21]. Besides, the calculations involved in this technique are computationally expensive, which makes real-time control even more difficult [22]. Indeed, even if there have been designed algorithms for external forces feedback as in [23], the high number of sensors and the complexity required are evident. Furthermore, ensuring that the robot can adapt to the timing of human actions, regardless of the viewing perspective, is fundamental to optimal interaction. In addition, recent advances have shown promising results in view-invariant robot adaptation to human action timing, essential for maintaining synchrony in joint tasks [24]. Moreover, drawing on insights from musculoskeletal modeling for gait analysis, using signal energy [25] as a measure of adaptation could provide a quantitative way to evaluate how efficiently the robotic system adapts to human input without deviating from the natural flow of interaction [26]. This metric highlights the robot’s ability to respond dynamically to human movements.

By addressing the limitations of non-adaptive behaviors and emphasizing the importance of compliance and social awareness in robots, this research focuses on developing a control strategy that better mimics human-like interactions, improving the effectiveness and naturalness of the physical collaborative sawing activity studied. The control strategy should prioritize algorithms that do not rely on force signals [27] to assess scalable real-world HRI systems. This approach should have to ensure efficient, responsive interactions without highly compromising the system’s performance in practical scenarios [28].

II. DESIGN AND METHODS

This chapter of our manuscript presents an adaptive control technique that dynamically adjusts impedance coefficients. The

main focus is to influence the iCub’s movement velocity. The controller integrates kinematic adjustments, compliance modulation, and real-time feedback, with key components related to movement phase transitions and motion synchronization. Moreover, the data analysis will concentrate on kinematic signals and soap indentation to evaluate interaction dynamics and task performance. Further, jerk energy has been used to quantify adaptation effort, distinguishing passive and active behaviors. The results will indicate whether our design achieves higher efficiency than a passive control method in executing a specific pHRI task.

Moreover, before exploring the design and the methods, it is important to define that in the specific context of our manuscript, the terms active and passive behavior assume a specific definition. The passive behavior is represented by a compliant controller that regulates the iCub’s arm movement, but with a fixed trajectory and velocity concerning the human participant’s actions. In contrast, the active behavior is defined by our novel approach, which, unlike the passive case, can respond to human stimuli and adjust the velocity of the iCub’s arm movements.

A. Participants

The required number of participants was determined through an a priori power analysis on the passive session task efficiency data for a Wilcoxon-Mann-Whitney test, assuming its similar non-normal distribution even for the active session. With an effect size of 0.8, $\alpha = 0.05$, and power = 0.8, the analysis indicated 21 participants per group. Given the designed active controller’s response to human stimuli, we expected a large effect size. Finally, to ensure robustness against acquisition errors and robot misbehavior, we increased the sample size aligning it with the passive session.

Thirty right-handed people participated in the study (12 females, 18 males; mean age = 25.30 y.o.; std = 3.58 y.o.). All participants were naive to the purpose of the study. The Regional Ethics Committee (Protocol: IIT_INT_HRI) approved the experimental protocol and all participants provided their written informed consent prior to starting the experiment.

B. Apparatus

The experimental setup, shown in Fig. 1, included the humanoid robot iCub, a steel wire with two handles, and a new soap bar for each participant supported in the middle of the peers during the duration of the task. The soap bars were equal for all the participants and identical to the one used in the passive behavior experiment. Half of the participants used the right hand, while the other half used the left hand to avoid the possible effects of using the dominant hand. The experimental session lasted four minutes, as suggested by human-human literature [29], during which participants and the experimenter could not interact. Every participant could perform only one experimental session without prior practice, and their unique objective was to collaborate with the iCub to maximize the soap cut.

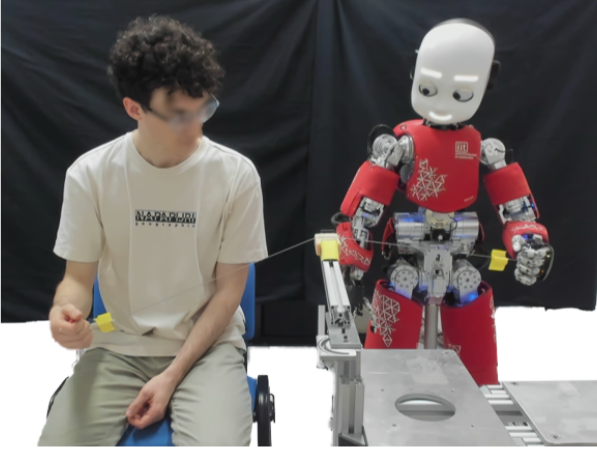


Fig. 1. Collaborative sawing task in pHRI. The experiment features a human-robot dyad engaged in a collaborative sawing task using a flexible steel wire to cut through a soft object, like a soap bar. Each participant alternately pulls the wire, necessitating synchronized movements and frequent adaptations in their coordination to maximize the cut depth.

C. Procedure

The experiment entails a human-robot dyad engaged in a collaborative physical joint task, specifically a sawing activity. Using a flexible steel wire, the participant and the robot work together to cut a soft object (e.g., a soap bar). Each party holds one handle of the wire, which requires coordination between the partners pulling in turns to maximize the indentation through the soap. A repetitive task in a physical collaboration, such as this one, leads to frequent changes and mutual adaptations in motion (e.g., the velocity of the movement, the spatial distance traveled, etc.). Thus, the robot iCub autonomously selects the appropriate timing for its action, adapting its motor control system to the human partner’s motor behavior. These changes are defined as *dynamic instants*, specifically referring to the change in the pulling phase between the human and the robot, indicated by a change in the direction of motion. This definition slightly differs from previous work [30], where these changes were defined in their temporal dynamics and exploited by observing variations in velocity, acceleration, and direction of motion (marked by null velocity). In addition, the term *baseline* will be found during the explanation of the experiment and data analysis to describe the output collected when the iCub performs the task alone, executing the cutting action movements without any external interference or stimuli. These data are useful for tracing differences between the default movements and trajectories handled, and those affected by the participant’s action.

D. Controlling Technique

The proposed control technique aims to facilitate natural and intuitive collaboration without neglecting task performance. Such a procedure dynamically adjusts the impedance controller coefficients based on real-time feedback. Therefore, the active behavior involves a mimic role responsive to human stimuli, modifying the impedance control coefficient upon receiving feedback. The compliance modality, integral to the impedance

controller, includes three levels: soft, medium, and hard, as suggested by the iCub’s software.

Fig. 2 shows the specific kinematic elements crucial to facilitating the creation of a cyclical exchange of forces. More specifically, Fig. 2(a) shows the adjustment of the default endpoint H to point H* moving toward the human direction. In addition, Fig. 2(b) illustrates the point R*, which aims to approach the baseline R as closely as possible to maximize the range of motion (ROM) of the iCub hand. For both those elements to be considered valid, the measured values shall surpass a predefined threshold greater than zero. Moreover, the trajectory’s relative velocity emerged as a promising variable for feedback in the controller design. This metric, which represents the ratio of the iCub’s hand movement from point R to point H relative to the time taken, requires evaluation during the participant’s phase. However, such a feedback approach introduces several critical points that require further analysis:

- 1) the presence of compliance yields lower steadiness in position reaching;
- 2) phase status should be evaluated in terms of both time and position;
- 3) the iCub’s contribution to task efficiency needs to be increased.

We selected soft and medium compliance levels as the controller definition boundaries for changes to address the first point. Initially, the experiment used time control to differentiate the pulling phases, which caused unwanted pauses between the human and robot phases. To address this issue, a spatial reference, evaluated as a semi-sphere centered in point H, is used to signify the end of the human phase and the beginning of the iCub’s pulling phase.

We considered the force exchange during a human dyad dynamic instant to address the second point. In this instant, one partner gradually releases force in human couples while the other increases it, following coordination timing. Hence, after reaching the semi-sphere, the compliance coefficient increases linearly starting from soft (see Formula (1)). This change prompts the participant to reduce their force, and when the velocity approaches zero, the iCub starts its pulling phase. The hypothesis is that the participant will perceive the iCub’s force increment as automatic coordination. Such a procedure is termed as **Dynamic Instant Manager**. The force increment enhances the robot’s contribution to the task, addressing the third point. Such an increment’s step size has to be configured experimentally to balance coordination naturalness. It shall be noticed that the radius of the semi-sphere around H has a fixed value equal to $A_y \cdot (105\% - 55\%)$. The constraint was established through experimental testing.

$$aC_i = aC_i + (mC_i - sC_i) \cdot \text{complianceStep} \quad (1)$$

$$\text{s.t.} \begin{cases} \text{complianceStep} = 1.45 - \frac{A_y^*}{A_y}, & 0.55 < \frac{A_y^*}{A_y} < 1.05 \\ \text{complianceStep} = 1, & \text{otherwise} \end{cases}$$

$$\text{where} \begin{cases} aC_i, mC_i \text{ and } sC_i \text{ are respectively the actual,} \\ \text{medium, and soft compliance constants values;} \\ A_y \text{ and } A_y^* \text{ are the baseline and the actual position} \\ \text{y-axis components.} \end{cases}$$

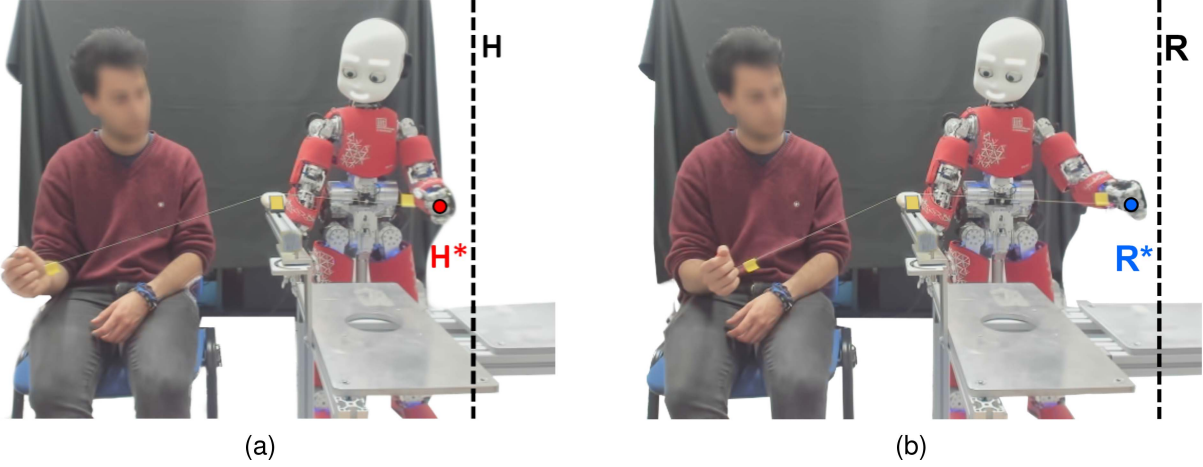


Fig. 2. Trajectory perturbation and positional deviations in the collaborative pHRI sawing task. The robot controls its hand movement between fixed points H and R (dotted lines in the figure). Due to the compliance in the robot's joints, coordination between peers leads to deviations from the predefined ideal positions, resulting in the measured positions H* and R*. Previous studies have shown that increasing trajectory deviations can facilitate collaboration's force exchange. (a) The perturbation of the trajectory toward the human's peripersonal space (from H to H*, shown by the red point). (b) A similar positional deviation occurs during the robot's pulling phase (from R to R*, shown by the blue point).

Afterward, the iCub's wire-pulling action must match the human peer's velocity to achieve the mimic effect, where a mutual collaboration due to spontaneous behavior arises from the interaction and is the key driver of synchronization, as there is neither a leader nor a follower. Given the non-solid interface connecting the participants (e.g., the flexible wire), a form of negotiation is necessary to achieve proper synchronization to maintain wire tension and generate friction to facilitate cutting. This condition was met by adjusting the damping and stiffness coefficients in Hooke's law [31]. The velocity of the iCub was measured, and the difference from the human's relative velocity was used as feedback for the controller. The feedback collection frequency was 100 Hz. This procedure evaluated using the formula (2) is referred to as the **Velocity Controller**.

$$aC_i = aC_i + (mC_i - sC_i) \cdot \text{updateRate} \cdot \left[\frac{v_{rH} - v_{rR}}{v_{toll}} \right] \quad (2)$$

where $\left\{ \begin{array}{l} \text{updateRate is the step of the stiffness and damping;} \\ v_{toll} \text{ is the experimentally chosen tolerance} \\ \text{underneath which no correction is made;} \\ v_{rH} \text{ and } v_{rR} \text{ are the relative velocities of human} \\ \text{and robot phase.} \end{array} \right.$

When the iCub's pulling phase approaches the final critical point, the compliance level affects whether the robot reaches a position near the baseline point (R) or earlier (R*). To manage this, a dynamic tolerance sphere around R adjusts its radius based on the compliance level (e.g., softer compliance results in a larger sphere radius). Until the iCub reaches this sphere, it will decrease the applied force, prompting the human to increase his force and start his pulling phase, thus restarting the cycle. The concept of the error sphere is illustrated in Fig. 3(a) and is sufficient for complete feedback control in position. The control algorithm was finalized by managing the arm's position

in Cartesian coordinates. The arm was set at a fixed angle of 35° relative to the horizontal axis, based on the robot's reference frame located in its torso. This adjustment aimed to mirror the movements of human partners observed during interactions. This detail represents the **Trajectory Planner** block, enhancing the iCub's contribution to the task.

In conclusion, Fig. 3(b) summarizes the design of the controller algorithm. The **Trajectory Planner** and **Dynamic Instant Manager** are a direct result of the experimental design, playing a crucial role in enhancing both the efficiency of the task and human participation in the collaborative process. The core of the controller is the **velocity controller**, which modulates the velocity and, by extension, the interaction force through the stiffness and damping parameters. This ensures smooth and coordinated motion by regulating the step response of the relative velocity during the human phase.

E. Data Analysis

The analyses in this research focus on multiple techniques used to evaluate the kinematic and physical aspects of the physical collaborative HRI. The analyses included the kinematic requirements for the force exchanged between the couple, the position and velocity signal evaluation to evaluate the dynamics, soap physical indentation examination to estimate the exerted contributions, and the jerk signal's energy measurement to assess the robot's adaptivity.

Data collection included kinematic signals from the iCub sensors and physical indentation measured from the soap bars. The kinematic data consisted of position signals rotated in the robot's hand reference frame. Our analyses focused on the horizontal and vertical components within the plane facing the iCub, specifically along the segment that connects the desired trajectory reaching points H and R in space. The collected signals were filtered to remove white noise and trimmed to exclude time intervals that exceeded the task duration. Then, maximum

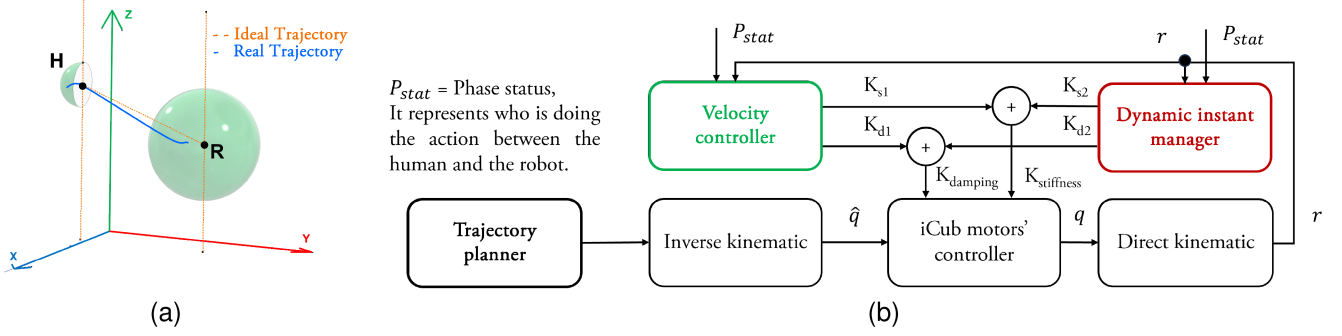


Fig. 3. Position tolerance and control schema for iCub’s active behavior. (a) Position control represented by the tolerance spheres. The semi-sphere of H has a fixed radius and applies force to stop the participant’s hand, marking the transition to the pulling phase. The sphere’s radius of R varies based on the robot’s compliance level during the pulling phase, with softer compliance resulting in a larger radius. The **Ideal Trajectory** (yellow dashed line) is perturbed by the compliance action, resulting in the **Real Trajectory** (blue line). (b) Control schema implemented for iCub’s active behavior. The original kinematic model governs joint control through inverse kinematics, generating joint angles for motor controllers and direct kinematics for cartesian feedback. Additional blocks define the active control strategy: the **Dynamic Instant Manager** slows down the human hand during the final phase of pulling; the **Trajectory Planner** adjusts the cutting angle and joint stiffness when transitioning from human to robot pulling phases; and the **Velocity Controller** manages the robot’s pulling phase by varying joint stiffness to replicate the human’s relative velocity.

and minimum peaks corresponding to the measured trajectory reaching points (H^* and R^*) were identified from the position signal to assess their characteristics, such as precise position, time phase shift, and relative velocity.

The data collected emphasized two main aspects: the comparison between passive and active behaviors and the relative velocity during each pulling phase. This focus on relative velocity is essential for understanding the interaction’s dynamics, which in turn aids in evaluating task efficiency. In addition, soap bar indentation areas were measured with a caliper on a fixed structure and reference frame, with multiple measurements taken to ensure repeatability and reproducibility. The data encompassed various aspects of the interaction, providing insight into the pHRI to contribute to task efficiency.

To gain a deeper understanding of this approach, we must assess the adjustments made between the human and the robot during their interaction. It is possible to quantify these adaptations by examining the jerk signal, which represents the rate of change in acceleration. This signal reflects the effort required for both the human and the robot to adjust their velocities and synchronize actions. This coefficient measures the intensity of effort exerted during the adaptations necessary to maintain the observed efficiency level, and is evaluated based on the difference between the velocities of humans and robots using formula (3).

$$j(t) = \frac{\delta(|v_H(t)| - |v_R(t)|)^2}{\delta^2 t},$$

where t is the number of phases. (3)

This calculation quantifies the variation between the two signals over time, indicating how quickly stability was achieved and describing the adaptability of the signals. To condense the time variation into a single coefficient per participant, following signal processing theory [25], the energy of the jerk (E_j) was

calculated using formula (4). E_j was evaluated for each experiment during the passive and active behavior sessions.

$$E_j = \sum_{n=0}^{Nphases} |j(n)|^2 \quad (4)$$

The energy signal undergoes a filtering approach that excludes the initial participant study phase and the final convergence of signals. Indeed, those time frames reflect the partners’ gained experience and coordination over time and shall not be adopted for the energy evaluation. The possible expected outcomes could lead to a higher energy requirement, indicating an adaptation process, or a lower energy requirement, indicating rapid convergence of one signal. In this study, the low energy for passive behavior represents a quick accustoming of the human to the robot’s fixed pace.

III. RESULTS

We used linear regression and independent t-tests for statistical analysis to compare the results of active and passive behavior. We excluded two participants from the study due to acquisition errors in kinematics features. The analyses included twenty-eight subjects (11 females, 17 males; mean age = 25.28 y.o.; std = 3.68 years).

The engagement of the parties in the collaborative task resulted first in a deviation of the position H towards H^* of a mean = 2.23 cm and std = 0.95 cm. Secondly, it expanded the size range of motion relative to the baseline value of a mean = 2.28 cm and std = 1.48 cm. The results of the Independent Samples T-Test confirmed that both coefficients were significantly greater than zero, with t-values of 8.15 and 12.40, respectively, resulting in p values less than 0.001. This statistical significance met the requirement criteria for the analysis, affirming that the range of motion size’s enlargement and the extension of the robot hand trajectory into the human peripersonal space satisfied the study requirements. Furthermore, the collected position signal was used to evaluate the relative velocity for both pulling phases,

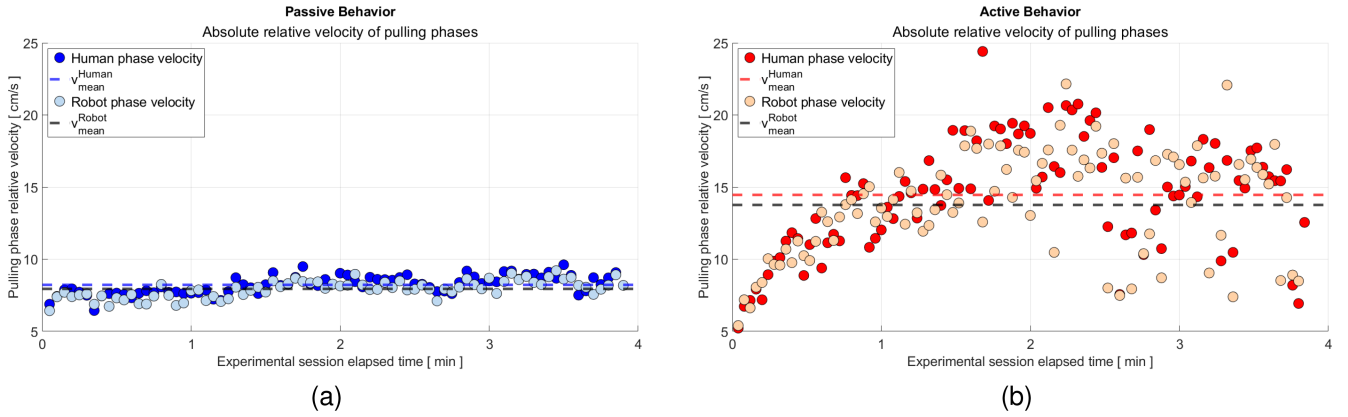


Fig. 4. Velocity dynamics during the collaborative sawing pHRI. (a) The robot’s phase velocity is fixed in passive behavior, requiring the human participant to adapt their strategy to match it. The static nature of the robot’s velocity emphasizes adaptability’s importance in achieving better results. (b) As the interaction progresses, the adaptive behavior of the iCub robot allows the human participant to increase their speed, achieving consistency around their preferred velocity after approximately half of the interaction time. This adjustment highlights the dynamic nature of human-robot interaction, as the iCub effectively synchronizes its pace to match its partner’s movements.

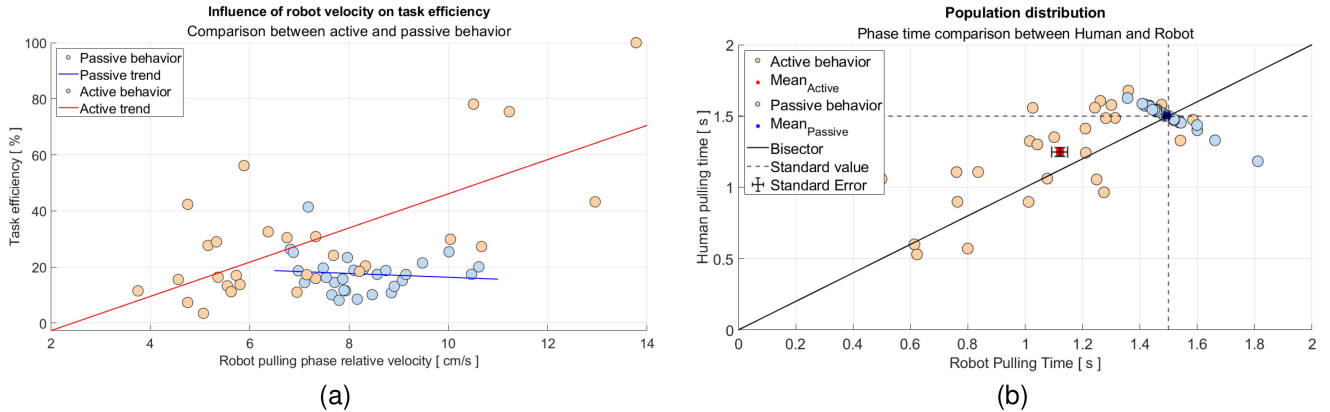


Fig. 5. Influence of robot velocity and behavior on task efficiency and synchronization. (a) The impact of robot velocity on task efficiency varies with the robot’s behavior type. As velocity increases, the active behavior significantly affects the removed material percentage more than the passive behavior. This result highlights the importance of growing velocity to maximize performance, with the active behavior achieving higher task efficiency at the same velocity. (b) Distribution of phase times for both peers. The passive behavior (blue dots) maintains a fixed value of around 1.5 s (the iCub’s phase time), while the active behavior adapts to individual partner preferences. Notice that iCub, with active behavior, adjusts its pace to match the partner’s timing, indicating improved synchronization and adaptability.

resulting in a $\text{meanH} = 6.76 \frac{\text{cm}}{\text{s}}$ and $\text{stdH} = 1.33 \frac{\text{cm}}{\text{s}}$ for the human peer, and a $\text{meanR} = 7.29 \frac{\text{cm}}{\text{s}}$ and $\text{stdR} = 1.20 \frac{\text{cm}}{\text{s}}$ for the iCub robot. Fig. 4 illustrates an example of the difference between the velocity signals of the passive and active behaviors. Lastly, the indentation percentages of soap bars, regarding the material removed in the area of a soap section, were measured with $\text{mean} = 29.28\%$ and $\text{std} = 23.00\%$.

The main result relates to the efficiency of the task. In fact, a linear regression analysis was conducted to examine the relationship between robot velocity and the amount of material removed, considering the type of robot demeanor (active versus passive), as shown in Fig. 5(a). The model explained a moderate proportion of the variation in the removed material ($R^2 = 0.503$). Significant predictors of removed material included robot velocity and the interaction between robot velocity and behavior. Specifically, in terms of active behavior, the robot velocity was positively associated with the removed material (active

behavior: $\beta = 6.10$, $p < 0.001$; passive behavior: $\beta = -0.678$, $p = 0.782$). The interaction term between velocity and behavior type was also significant ($\beta = 6.78$, $p = 0.012$), indicating that the effect of velocity on material removal differed between active and passive behaviors. These results suggested that higher velocity leads to greater task efficiency and is moderated by the type of demeanor, with a more pronounced result observed under the active behavior condition. Furthermore, the Mann-Whitney U Independent Single Tail T-Test confirmed the different distribution of performance in material removal: $U(28) = 272.00$, $p = 0.025$, $r_{rb} = 0.306$.

However, a question remains: did the people in the adaptive behavior session truly adapt? This was assessed by examining the average phase time of the population with the two behaviors, as shown in Fig. 5(b). In addition, the jerk energy coefficient was considered to quantify adaptability. The results of the jerk energy (passive behavior: $\text{mean} = 0.006 \frac{\text{cm}^2}{\text{s}^3}$, $\text{std} = 0.006 \frac{\text{cm}^2}{\text{s}^3}$,

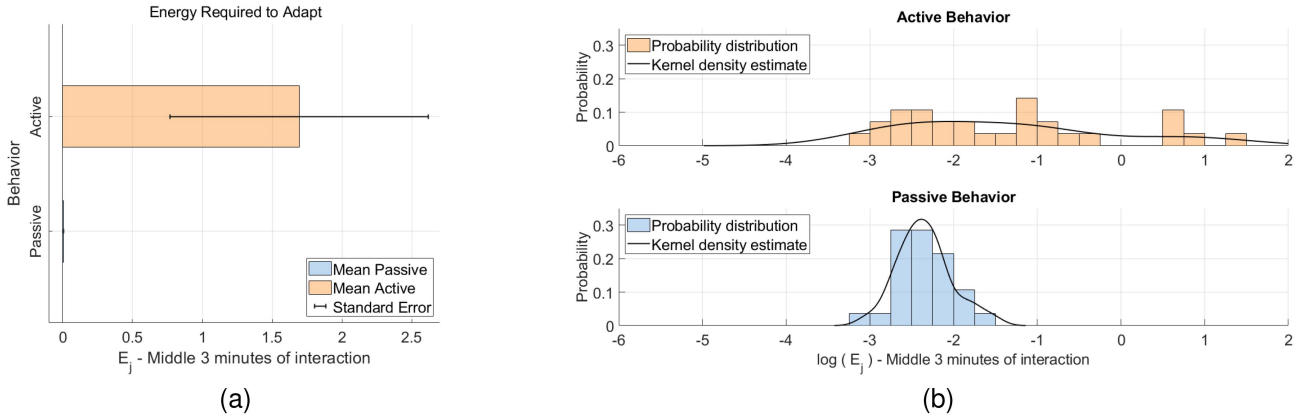


Fig. 6. Energy required for the peers to adapt to each other. (a) The energy expenditure in the active case is substantially higher (approximately ten times greater) than in the passive case. (b) The logarithmic scale of the probability distribution highlights the magnitude difference between the two behaviors. Specifically, it shows that active behavior spreads energy demand across various high-energy areas, while passive behavior is confined to a narrower, less energy-intensive range. This distribution pattern enhances adaptability in active behavior, making it particularly effective in situations like adapting to varying human fatigue levels.

active behavior: mean = $1.693 \frac{cm^2}{s^3}$, std = $4.900 \frac{cm^2}{s^3}$) are shown in Fig. 6, while the independent sample T-test amounts to: $t(28) = 205.00$, $p = 0.002$, $r_{rb} = 0.477$. These higher energy values in active behavior suggested that more effort was required to achieve adaptation between human and robot. Indeed, the passive behavior did not leave room for adaptation due to the fixed robot behavior, thus, no effort was needed to reach the synchronization. In support of this result, the jerk energy measured was much lower than in the active demeanor. Although such an energy expenditure indicated that task performance improved during active behavior, it also highlighted the increased effort needed to sustain this performance.

IV. DISCUSSION AND FUTURE WORK

This work highlights the critical components of performance in collaborative physical HRI, studying the dynamic environment of co-manipulation tasks [14], for different Human-Robot co-actions [32]. In particular, the principal objective was to design a control technique that would increase task efficiency in a joint human-robot sawing task without using a force feedback control approach. Previous implementations used a passive control design that enabled collaborative pHRI through compliance, allowing the robot to accommodate perturbations along its trajectory. However, this approach had limitations in activity performance due to its static nature and inability to adapt to human stimuli and needs. Thus, a focused investigation of the outcome of this control technique was imperative, prompting an analysis of the physical collaborative action and the development of a control design that not only maintains the participation of the human partner but also overcomes a limitation of previous methods. Implementing an active behavior for the robot successfully demonstrated the desired dynamics between the human and the robot in this task, highlighting the essential role of force exchange in allowing the human to influence the trajectory of the robot. As the iCub robot transitioned from passive to active behavior, it increased its contribution to the action through adaptive force and velocity adjustments,

emphasizing its ability to respond dynamically to human action changes. We showed that the applied control strategy, which utilized Cartesian impedance control and adjustments based on Hooke's law, improved task efficiency. This method allowed the robot to account for the human participant's varying velocities and fatigue levels. In addition, by measuring the jerk energy, we proved that active behavior required more energy consumption, which enhanced performance. This underscores the importance of balancing effort intensity with task efficiency in human-robot collaboration.

The main limitation of our current work concerns the temporal dynamics of the robot's adaptability to human stimuli. During the initial phase of the step response, the settling time is difficult to control, even after numerous calibration tests. This is because the generation of the response to the step is done with a linear function regulated by an increasing step variable. The step function to follow generates significant step differences between two human pulling phases, and the combination of settling time and overshoot is insufficient to reach the desired velocity precisely. We pinpoint that this issue arises because the controller is acting to correct a parameter indirectly, that is, changing the velocity using the stiffness and damping coefficients.

The planned future work involves the design of a formula that can connect the velocity and Hooke's law coefficients correctly without affecting the inertia matrices. In fact, modification of inertia matrices is a technique extensively explored in the admittance controller of manipulator robots [33], [34], though still limited in applications for humanoid robots equipped with precise force/torque (F/T) sensors [35] or even sensorless [36]. In addition, the dynamic findings shall be integrated with social factors to enhance human perception of the robot.

Our study advanced the understanding of human-robot collaboration by demonstrating how active control strategies improved the efficiency of co-manipulative tasks. The integration of adaptive force and velocity adjustments showcased an efficient alternative to traditional force-feedback controls. The findings emphasized adaptability's significance in physical human-robot interaction, providing a foundation for further exploration of

dynamic behaviors and their effects on human perception and task performance in collaborative settings.

ACKNOWLEDGMENT

This work has been carried out within the Brain and Machines Flagship of the Italian Institute of Technology.

REFERENCES

- [1] A. Sciutti, M. Mara, V. Tagliasco, and G. Sandini, "Humanizing human-robot interaction: On the importance of mutual understanding," *IEEE Technol. Soc. Mag.*, vol. 37, no. 1, pp. 22–29, Mar. 2018.
- [2] R. P. Van der Wel, G. Knoblich, and N. Sebanz, "Let the force be with us: Dyads exploit haptic coupling for coordination," *J. Exp. Psychol., Hum. Percept. Perform.*, vol. 37, no. 5, 2011, Art. no. 1420.
- [3] T. L. Chartrand and J. A. Bargh, "The chameleon effect: The perception–behavior link and social interaction," *J. Pers. Social Psychol.*, vol. 76, no. 6, 1999, Art. no. 893.
- [4] S. Kashi and S. Levy-Tzedek, "Smooth leader or sharp follower? Playing the mirror game with a robot," *Restorative Neurol. Neurosci.*, vol. 36, no. 2, pp. 147–159, 2018.
- [5] A. Takagi, F. Usai, G. Ganesh, V. Sanguineti, and E. Burdet, "Haptic communication between humans is tuned by the hard or soft mechanics of interaction," *PLoS Comput. Biol.*, vol. 14, no. 3, 2018, Art. no. e1005971.
- [6] Y. Liu, X. Chen, Z. Yu, H. Yu, L. Meng, and H. Yokoi, "High-precision dynamic torque control of high stiffness actuator for humanoids," *ISA Trans.*, vol. 141, pp. 401–413, 2023.
- [7] S. Regmi, D. Burns, and Y. S. Song, "Humans modulate arm stiffness to facilitate motor communication during overground physical human-robot interaction," *Sci. Rep.*, vol. 12, no. 1, 2022, Art. no. 18767.
- [8] A. Melendez-Calderon, V. Komisar, G. Ganesh, and E. Burdet, "Classification of strategies for disturbance attenuation in human-human collaborative tasks," in *Proc. 2011 Annu. Int. Conf. IEEE Eng. Med. Biol. Soc.*, 2011, pp. 2364–2367.
- [9] N. Jarrasse, V. Sanguineti, and E. Burdet, "Slaves no longer: Review on role assignment for human–robot joint motor action," *Adaptive Behav.*, vol. 22, no. 1, pp. 70–82, 2014.
- [10] A. Tanevska, F. Rea, G. Sandini, L. Cañamero, and A. Sciutti, "A socially adaptable framework for human-robot interaction," *Front. Robot. AI*, vol. 7, no. 121, 2020.
- [11] G. Hoffman and C. Breazeal, "Effects of anticipatory action on human-robot teamwork efficiency, fluency, and perception of team," in *Proc. ACM/IEEE Int. Conf. Hum.-Robot Interaction*, 2007, pp. 1–8.
- [12] G. Scorza Azzarà, J. Zonca, F. Rea, J.-H. Song, and A. Sciutti, "Biased attention near iCub's hand after collaborative HRI," in *Proc. Companion 2024 ACM/IEEE Int. Conf. Hum.-Robot Interact.*, 2024, pp. 970–974.
- [13] T. Lorenz, A. Mörtl, and S. Hirche, "Movement synchronization fails during non-adaptive human-robot interaction," in *Proc. 8th ACM/IEEE Int. Conf. Hum.-Robot Interaction*, 2013, pp. 189–190.
- [14] A. Tiozzo, "Exploiting the adaptability of the humanoid robot iCub to personalize a physical human-robot interaction," Master's thesis, Polytechnic Turin, Turin, Italy, 2024.
- [15] G. Scorza Azzarà et al., "Creation of a joint body schema in human-robot interaction: Investigating the kinematic features of a physical collaboration," in *Proc. ACM/IEEE Int. Conf. Hum.-Robot Interaction*, unpublished.
- [16] H.-M. Sun and L. E. Thomas, "Biased attention near another's hand following joint action," *Front. Psychol.*, vol. 4, no. 443, 2013.
- [17] A. Roncone, M. Hoffmann, U. Pattacini, L. Fadiga, and G. Metta, "Peripersonal space and margin of safety around the body: Learning visuo-tactile associations in a humanoid robot with artificial skin," *PLoS one*, vol. 11, no. 10, 2016, Art. no. e0163713.
- [18] A. Vasalya, G. Ganesh, and A. Kheddar, "More than just Co-workers: Presence of humanoid robot Co-worker influences human performance," *PLoS one*, vol. 13, no. 11, 2018, Art. no. e0206698.
- [19] R. C. Schmidt, P. Fitzpatrick, R. Caron, and J. Mergeche, "Understanding social motor coordination," *Hum. Movement Sci.*, vol. 30, no. 5, pp. 834–845, 2011.
- [20] S. Gopinathan, S. K. Ötting, and J. J. Steil, "A user study on personalized stiffness control and task specificity in physical human–robot interaction," *Front. Robot. AI*, vol. 4, no. 58, 2017.
- [21] G. Metta, G. Sandini, D. Vernon, L. Natale, and F. Nori, "iCub: The design and realization of an open humanoid platform for cognitive and neuroscience research," *Adv. Robot.*, vol. 21, no. 10, pp. 1151–1175, 2010.
- [22] V. Mattioni, E. Ida', and M. Carricato, "Design of a planar cable-driven parallel robot for non-contact tasks," *Appl. Sci.*, vol. 11, no. 20, 2021, Art. no. 9491.
- [23] M. Fumagalli et al., "Force feedback exploiting tactile and proximal force/torque sensing: Theory and implementation on the humanoid robot iCub," *Auton. Robots*, vol. 33, pp. 381–398, 2012.
- [24] N. Noceti, F. Odone, F. Rea, A. Sciutti, and G. Sandini, "View-invariant robot adaptation to human action timing," in *Proc. Intell. Syst. Appl.*, 2019, vol. 1, pp. 804–821.
- [25] W. Alexander and C. M. Williams, "Chapter 2-fundamental DSP concepts," in *Digital Signal Processing: principles, algorithms and system design*. Academic Press, 2016, pp. 19–157.
- [26] M. Abdullah, A. A. Hulleck, R. Katmah, K. Khalaf, and M. El-Rich, "Multibody dynamics-based musculoskeletal modeling for gait analysis: A systematic review," *J. NeuroEngineering Rehabil.*, vol. 21, no. 1, 2024, Art. no. 178.
- [27] S. Huang, K. Koyama, M. Ishikawa, and Y. Yamakawa, "Human-robot collaboration with force feedback utilizing bimanual coordination," in *Proc. Companion 2021 ACM/IEEE Int. Conf. Hum.-Robot Interaction*, 2021, pp. 234–238.
- [28] A.-N. Sharkawy and P. N. Koustoumpardis, "Human–robot interaction: A review and analysis on variable admittance control, safety, and perspectives," *Machines*, vol. 10, no. 7, 2022, Art. no. 591.
- [29] T. M. Soliman, R. Ferguson, M. S. Dexheimer, and A. M. Glenberg, "Consequences of joint action: Entanglement with your partner," *J. Exp. Psychol., Gen.*, vol. 144, no. 4, pp. 873–888, 2015.
- [30] F. Rea, A. Vignolo, A. Sciutti, and N. Noceti, "Human motion understanding for selecting action timing in collaborative human-robot interaction," *Front. Robot. AI*, vol. 6, no. 58, 2019.
- [31] J. O. Thompson, "Hooke's law," *Science*, vol. 64, no. 1656, pp. 298–299, 1926.
- [32] Y. Shao, T. Li, S. Keyvanian, P. Chadhuari, V. Kumar, and N. Figueroa, "Constraint-aware intent estimation for dynamic human-robot object co-manipulation," in *Proc. Robot., Sci. Syst.*, 2024.
- [33] Y. Aydin, D. Sirintuna, and C. Basdogan, "Towards collaborative drilling with a cobot using admittance controller," *Trans. Inst. Meas. Control*, vol. 43, no. 8, pp. 1760–1773, 2021.
- [34] E. Mariotti, E. Magrini, and A. De Luca, "Admittance control for human-robot interaction using an industrial robot equipped with a F/T sensor," in *Proc. 2019 Int. Conf. Robot. Automat.*, 2019, pp. 6130–6136.
- [35] Y. M. Hamad, Y. Aydin, and C. Basdogan, "Adaptive human force scaling via admittance control for physical human-robot interaction," *IEEE Trans. Haptics*, vol. 14, no. 4, pp. 750–761, Oct.–Dec. 2021.
- [36] J. Cho, D. Choi, and J. H. Park, "Sensorless variable admittance control for human–robot interaction of a dual-arm social robot," *IEEE Access*, vol. 11, pp. 69366–69377, 2023.